SCIENCE CHINA
Information Sciences

• RESEARCH PAPER •

July 2023, Vol. 66 172202:1–172202:15
https://doi.org/10.1007/s11432-022-3632-2

Fault detection and isolation for linear parameter-varying systems with time-delays: a geometric approach

Zhao ZHANG & Xiao HE*

Department of Automation, Tsinghua University, Beijing 100084*, China*

Received 23 July 2022/Revised 27 September 2022/Accepted 18 November 2022/Published online 9 May 2023

Abstract Fault detection and isolation (FDI) problems for linear parameter-varying (LPV) systems with state time-delays are studied in this paper. By defining the concept of unobservability subspace and designing its calculation algorithm, the geometric approach is introduced to the time-delay LPV systems. Utilizing Wirtinger-based integral inequality, we obtain a sufficient condition to solve the so-called H_∞-based residual generation problem for the LPV systems. In this paper, we consider two cases: the time delay is known and the time delay is unknown but its estimated value can be obtained. Corresponding observers are proposed for both cases based on the geometric approach and H_∞ techniques. Lyapunov-Krasovskii functional is utilized to handle the time-delays and Wirtinger's inequality is employed to reduce conservatism. Numerical examples are presented to demonstrate the effectiveness of the proposed approach.

Keywords time-delay LPV systems, geometric approach, fault detection and isolation, exact-memory, rough-memory

Citation Zhang Z, He X. Fault detection and isolation for linear parameter-varying systems with time-delays: a geometric approach. Sci China Inf Sci, 2023, 66(7): 172202, https://doi.org/10.1007/s11432-022-3632-2

1 Introduction

System faults may pose severe challenges to the safety of the system and lead to disastrous consequences. In some safety-critical systems, such as aerospace, deep-sea manned submersible, high-speed aircraft, and chemical processes, safety and reliability are important factors for system design and operation [1–5]. Therefore, it is necessary to carry out fault diagnosis, which can provide fault information for subsequent operations (e.g., fault-tolerant controllers) to eliminate or weaken the impact of faults [6–10]. Driven by the actual industrial demand, fault diagnosis has become an important research topic in the field of automatic control. In the past decades, researchers have carried out extensive research on fault diagnosis techniques and published a series of results in this area [11–15].

The time-delay linear parameter-varying (LPV) system has the characteristics of both LPV systems and the time-delay phenomenon, and it has a wide range of applications in practice [16–20]. Many practical systems can be modeled as time-delay LPV systems. Han et al. [21] utilized the time-delay LPV system to establish a model of the supercavitating vehicle and designed a robust predictive controller. Tasoujian et al. [22] adopted the state-delay LPV system to describe the mean arterial blood pressure dynamics, and they used the Bayesian-based multiple-model square-root cubature Kalman filtering approach to estimate the varying parameters and delay. Zhang et al. [23] modeled the milling process as a time-delay LPV system and analyzed the system stability. It can be seen that the study of time-delay LPV systems is of wide practical importance. However, most existing results are about system controller design, and there is a lack of research on fault diagnosis.

In terms of fault diagnosis of time-delay LPV systems, some research results have been published. Hassanabadi et al. [24] designed a proportional-integral unknown input observer to estimate the actuator

* Corresponding author (email: hexiao@tsinghua.edu.cn)

fault for singular delayed LPV systems. Hamdi et al. [25] proposed an adaptive polytopic observer to detect time-varying faults. Combined with set theory, a set-theoretic unknown input observer was put forward for robust fault detection for LPV systems in [26]. In most existing results, a common assumption is that only one fault occurs at the same time. The main purpose is to detect whether the fault occurs or estimate the fault amplitude. When there are multiple faults in the system, the mentioned methods cannot effectively isolate different faults. In linear time-invariant systems, an effective fault detection and isolation (FDI) method is the geometric fault observer, which was proposed by Massoumnia et al. [27,28]. Thanks to the excellent properties of the geometric fault observer, it has been generalized to solve the FDI problems for LPV systems by Bokor et al. [29,30]. However, they did not consider time-delays, and to the best of the author's knowledge, there have been no results in introducing the geometric approach to time-delay LPV systems. The analysis and design of geometric approach-based FDI observers for time-delay LPV systems is still a challenging problem.

In response to the above discussions, we consider the FDI problem for time-delay LPV systems in this paper to handle the following challenges: (1) How to introduce the geometric concepts to time-delay LPV systems for detecting and isolating multiple faults? (2) How to deal with the influence of time-delays on observer design? The basic goal of this paper is to provide a satisfactory solution to the above two questions. The main contributions of this paper are summarized as follows: (1) We propose the concepts of time-delay parameter-varying conditioned invariant subspace (TPCIS) and time-delay parameter-varying unobservability subspace (TPUS), and put forward their calculation algorithms. The geometric approach is successfully introduced to the time-delay LPV systems. (2) We consider two cases where the time-delay is known and the time-delay is unknown but its estimated value can be obtained. Fault diagnosis observers are designed for both cases based on the geometric approach and H_∞ techniques, respectively. (3) Lyapunov-Krasovskii functional is utilized to handle the time-delays and Wirtinger's inequality is employed to reduce conservatism.

The rest of the paper is outlined as follows. In Section 2, we formulate the considered problem. Section 3 introduces the concepts of TPCIS and TPUS and their geometric properties. Next, we design a set of FDI observers based on the geometric approach together with H_∞ techniques and obtain the sufficient conditions in Section 4 with the assumption that the time-delay is precisely known and the time-delay is unknown, respectively. The effectiveness of the proposed approach is illustrated through two numerical simulations in Section 5. Finally, we conclude this paper in Section 6.

Notation. Script letters, e.g. $\mathcal{X}, \mathcal{Y}$, represent real vector spaces. X^{-r} stands for the right inverse of X. $\mathcal{L}$ is used to refer to the range of L and $\ker C$ refers to the kernel space of C. $P \succ 0$ represents that P is symmetric and positive definite. For any square matrix $X \in \mathbb{R}^{n\times n}$, $\mathrm{He}(X) = X + X^{\mathrm{T}}$. The mark $*$ is used to represent a matrix that can be complemented by symmetry. $\|x\|_{L_2} = \left(\int_0^\infty x^{\mathrm{T}}(t)x(t)\mathrm{d}t\right)^{1/2}$ is the L_2-norm of $x(t)$. $\mathcal{X}^\perp$ denotes the orthogonal complement of subspace $\mathcal{X}$. $\boldsymbol{k}$ is defined as the set $\{1, 2, \ldots, k\}$. A matrix $X(\rho(t))$ is said to be an affine function with respect to $\rho(t)$ if it can be described as $X(\rho(t)) = X_0 + \rho_1(t)X_1 + \cdots + \rho_{n_\rho}(t)X_{n_\rho}$. The notation $\mathrm{diag}(A, B)$ represents a block diagonal matrix composed of A and B.

2 Problem formulation

Consider the following state time-delay LPV system:

$$\begin{aligned}
&\dot{x}(t) = A(\rho(t))x(t) + A_\tau(\rho(t))x(t-\tau(t)) + B(\rho(t))u(t) + B^d(\rho(t))d(t) + \sum_{i=1}^{k} L_i(\rho(t))m_i(t),\\
&y(t) = Cx(t) + D^d d(t),\\
&x(\theta) = \phi(\theta),\ \theta \in [-\tau_M,\, 0],
\end{aligned} \tag{1}$$

where $x \in \mathcal{X}$ is the state with dimension n_x, $y \in \mathcal{Y}$ is the output with dimension n_y, $u(t)$ is the input with dimension n_u, and $d(t)$ is the disturbance with dimension n_d. $m_i \in \mathcal{M}_i$, $i \in \boldsymbol{k}$ is the fault mode with dimension n_m^i, and $L_i(\rho(t))$ is the fault signature that is affine with respect to the scheduling parameters. Without loss of generality, we consider that there are k possible faults. $\tau(t)$ denotes the time-varying delay with $\tau(t) \in [\tau_m,\, \tau_M]$, where τ_m and τ_M are the minimal and maximal values of possible delays. The output matrix C is right invertible, D^d is a constant matrix, and system matrices $A(\rho(t)), A_\tau(\rho(t))$,

$B(\rho(t))$, and $B^d(\rho(t))$ are all affine functions. $\rho_i(t), i = 1, \ldots, n_\rho$ denotes the time-varying parameter. It is assumed that each parameter $\rho_i(t)$ varies between known extremal values $\rho_i(t) \in [\underline{\rho_i}, \bar{\rho}_i]$. The parameter set, which consists of all vectors $\rho(t) \triangleq [\rho_1(t), \ldots, \rho_{n_\rho}(t)], t \in [t_0, t_1]$, is defined as $\mathcal{P}$. For convenience and simplicity of expression, we use ρ to represent $\rho(t)$.

Assumption 1. It is assumed that the time-varying parameters are unknown but the current values can be obtained in real time.

Assumption 2. The disturbance signal $d(t)$ is L_2-norm bounded.

Assumption 3. The time delay $\tau(t)$ is time-varying and satisfies the following constraints:

$$\tau(t) \in [\tau_m, \tau_M], \ \ \dot{\tau}(t) \in [\varsigma_m, \varsigma_M], \ \ \forall t \geqslant 0, \tag{2}$$

where $0 \leqslant \tau_m \leqslant \tau_M$ and $\varsigma_m \leqslant \varsigma_M < 1$.

The main objective of this paper is to detect and isolate different faults for time-delay LPV systems based on the geometric approach. To achieve this goal, we need first to propose the basic geometric concepts including TPCIS and TPUS, and introduce the geometric approach to time-delay LPV systems. Based on the geometric approach together with H_∞ techniques, a set of observers will be designed to detect and isolate different faults.

3 Unobservability subspace

In this section, some relevant concepts in the geometric approach, including invariant subspace and unobservability subspace of state time-delay LPV systems, are summarized.

Definition 1. A subspace $\mathcal{V}$ is called a state time-delay parameter-varying invariant subspace (TPIS) for the family of linear maps $A(\rho)$ and $A_\tau(\rho)$ (denoted by $[A(\rho), A_\tau(\rho)]$-invariant subspace) if

$$A(\rho)\mathcal{V} \subseteq \mathcal{V}, \ A_\tau(\rho)\mathcal{V} \subseteq \mathcal{V}, \ \forall \rho \in \mathcal{P}. \tag{3}$$

The following lemma is useful for introducing the unobservability subspace for the state time-delay LPV systems.

Lemma 1 ([31])**.** Any state trajectory $x(t), t \in [t_0, t_1]$ belongs to a subspace $\mathcal{L} \subseteq \mathcal{X}$ if and only if $x(t_0) \in \mathcal{L}$ and $\dot{x}(t) \in \mathcal{L}$ almost everywhere (a.e.) in $[t_0, t_1]$.

Based on Lemma 1, we have the following result.

Lemma 2. Consider the following LPV system with state time-delays:

$$\begin{aligned} &\dot{x}(t) = A(\rho)x(t) + A_\tau(\rho)x(t - \tau(t)), \\ &x(\theta) = \phi(\theta), \ \ \theta \in [-\tau_M, 0]. \end{aligned} \tag{4}$$

Let $\mathcal{V} \subseteq \mathcal{X}$ be a $[A(\rho), A_\tau(\rho)]$-invariant subspace for all $\rho \in \mathcal{P}$. If $\phi(\theta) \in \mathcal{V}, \forall \theta \in [-\tau_M, 0]$, then $x(t) \in \mathcal{V}$ a.e. for $t \geqslant 0$.

Proof. First, let us show that if $\phi(\theta) \in \mathcal{V}, \forall \theta \in [-\tau_M, 0]$, then $\dot{\phi}(\theta) \in \mathcal{V}, \forall \theta \in [-\tau_M, 0]$. It is known that a Lebesgue measurable and integrable function is zero a.e. in $[t_0, t_1]$ if and only if its integral in any subinterval of $[t_0, t_1]$ is zero. By applying this property to the function $Y^{\mathrm{T}}\dot{\phi}(\theta)$, where Y is a basis of the subspace $\mathcal{V}^\perp$, we can get

$$\int_{-\tau_M}^{\theta} Y^{\mathrm{T}}\dot{\phi}(\theta)\mathrm{d}t = Y^{\mathrm{T}}(\phi(\theta) - \phi(-\tau_M)) = 0.$$

This indicates that $\dot{\phi}(\theta) \in \mathcal{V}, \theta \in [-\tau_M, 0]$ holds a.e.. In addition, $\dot{x}(0^+) = A(\rho)x(0) + A_\tau(\rho)x(-\tau(t)) \in \mathcal{V}$. Based on Lemma 1, we have $x(0^+) \in \mathcal{V}$. Similarly, it can be shown that $x(t) \in \mathcal{V}, t \geqslant 0$ by successive application of this process. This concludes the proof.

Remark 1. Meskin et al. [32, 33] proposed similar results for linear time-delay systems. Inspired by these studies, we put forward Lemma 2 for LPV time-delay systems.

Without loss of generality, we ignore the system input and disturbance when introducing the geometric concepts. In general, the following observers are designed to detect system faults:

$$\begin{aligned} &\dot{\hat{x}}(t) = A(\rho)\hat{x}(t) + A_\tau(\rho)\hat{x}(t - \tau(t)) + D(\rho)(\hat{y}(t) - y(t)) + D_\tau(\rho)(\hat{y}(t - \tau(t)) - y(t - \tau(t))), \\ &\hat{y}(t) = C\hat{x}(t), \\ &\hat{x}(\theta) = \phi(\theta), \ \ \theta \in [-\tau_M, 0], \end{aligned} \tag{5}$$

where $D(\rho)$ and $D_\tau(\rho)$ are observer matrices with affine form.

In general, $e(t) = \hat{x}(t) - x(t)$ is set to represent the estimation error. The residual can be designed as a linear mixture of the estimation error, that is, $r(t) = H(\hat{y}(t) - y(t))$. The dynamic equation of the residual can be obtained as follows:

$$\dot{e}(t) = (A(\rho) + D(\rho)C)e(t) + (A_\tau(\rho) + D_\tau(\rho)C)e(t - \tau(t)) - \sum_{i=1}^{k} L_i(\rho)m_i(t),$$
$$r(t) = HCe(t).$$

As can be seen in Section 4, the unobservability subspace plays an important role in the FDI problem of time-delay LPV systems. Aiming to introduce the definition of unobservability subspace, we first introduce the notation of TPCIS for given pairs of matrices $(C, A(\rho), A_\tau(\rho))$.

Definition 2. A subspace $\mathcal{W} \subseteq \mathcal{X}$ is called a TPCIS for the pairs of the linear maps C, $A(\rho)$, and $A_\tau(\rho)$ (denoted by $[C, A(\rho), A_\tau(\rho)]$-invariant subspace) if any one of the following equivalent conditions holds:

(1) For $\forall \rho \in \mathcal{P}$,

$$A(\rho)(\mathcal{W} \cap \ker C) \subseteq \mathcal{W},\ A_\tau(\rho)(\mathcal{W} \cap \ker C) \subseteq \mathcal{W}.$$

(2) There exist matrices $D(\rho)$ and $D_\tau(\rho)$ such that for $\forall \rho \in \mathcal{P}$,

$$(A(\rho) + D(\rho)C)\mathcal{W} \subseteq \mathcal{W},\ (A_\tau(\rho) + D_\tau(\rho)C)\mathcal{W} \subseteq \mathcal{W}.$$

Remark 2. The equivalence of the two conditions in Definition 2 can be proved through a similar method as in Subsection 4.1 in [31], which is omitted here.

Let $\mathcal{S} \subseteq \mathcal{X}$ be the largest $[C, A(\rho), A_\tau(\rho)]$-invariant subspace that is contained in $\ker HC$. According to Lemmas 1 and 2, for any initial condition $\phi(\theta) \in \mathcal{S}$, $\forall \theta \in [-\tau_M, 0]$, we have $r(t) = 0$, $\forall t \geqslant 0$ when there is no fault. Based on this conclusion, we define the notion of parameter-varying unobservability subspace for the time-delay LPV systems as follows.

Definition 3. A subspace $\mathcal{S} \subseteq \mathcal{X}$ is called a TPUS for the state time-delay LPV system (denoted by $[C, A(\rho), A_\tau(\rho)]$-unobservability subspace) if there exist output injection maps $D(\rho)$ and $D_\tau(\rho)$ and measurement mixing map H such that for $\forall \rho \in \mathcal{P}$,

$$\mathcal{S} = \langle \ker HC | A(\rho) + D(\rho)C,\ A_\tau(\rho) + D_\tau(\rho)C \rangle, \tag{6}$$

where $\langle \ker HC | A(\rho) + D(\rho)C,\ A_\tau(\rho) + D_\tau(\rho)C \rangle$ denotes the largest $[C, A(\rho), A_\tau(\rho)]$-invariant subspace that is contained in $\ker HC$. Based on this definition, we can see that unobservability subspace $\mathcal{S}$ is related to maps $D(\rho)$, $D_\tau(\rho)$, and H. For a given unobservability subspace $\mathcal{S}$, the map H can be calculated by the equation $\ker HC = \ker C + \mathcal{S}$.

Remark 3. According to Definitions 2 and 3, TPCIS and TPUS are subspaces that are determined by system matrices C, $A(\rho)$, and $A_\tau(\rho)$. The construction and properties of these subspaces are not affected by system disturbances.

It can be found that the unobservability subspace is a $[A(\rho) + D(\rho)C, A_\tau(\rho) + D_\tau(\rho)C]$-invariant subspace, and it is contained in $\ker HC$. Based on this property, we give a brief illustration of the geometric approach. Suppose we want to detect and isolate the i-th fault m_i among all the possible k faults. Then if there exists an unobservability subspace that contains all the other fault spaces, we can design a suitable observer such that the effects of all the other faults remain zero in the residual. Thus, we can successfully detect and isolate the i-th fault.

From the perspective of practical application, it is an important requirement to describe the characteristics of the above subspaces with a limited number of conditions. If we assume that matrices $A(\rho)$ and $A_\tau(\rho)$ satisfy affine structure, it is obvious that if the conditions hold for all A_i and $A_{\tau,i}$, then they also hold for all $A(\rho)$ and $A_\tau(\rho)$, $\forall \rho \in \mathcal{P}$.

Lemma 3 ([29])**.** Assume that the functions $\rho_i(t)$, $i = 1, \ldots, n_\rho$ are linearly independent. Then for any subspaces $\mathcal{V}_1$, $\mathcal{V}_2$, and affine function $A(\rho)$, $A(\rho)\mathcal{V}_1 \subseteq \mathcal{V}_2$ holds for $\forall \rho \in \mathcal{P}$ if and only if

$$A_i\mathcal{V}_1 \subseteq \mathcal{V}_2,\ i = 0, \ldots, n_\rho. \tag{7}$$

We employ $\underline{D}(\rho)(\mathcal{W})$ and $\underline{D_\tau}(\rho)(\mathcal{W})$ to represent the family of all maps $D(\rho)$ and $D_\tau(\rho)$ satisfying $(A(\rho)+D(\rho)C)\mathcal{W}\subseteq\mathcal{W}$ and $(A_\tau(\rho)+D_\tau(\rho)C)\mathcal{W}\subseteq\mathcal{W}$, respectively. Suppose $\mathcal{L}\subseteq\mathcal{X}$ is a subspace. Let $\underline{\mathcal{W}}(\mathcal{L})$ denote the class of $[C,\ A(\rho),\ A_\tau(\rho)]$-invariant subspaces containing $\mathcal{L}$. It should be pointed out that $\underline{\mathcal{W}}(\mathcal{L})$ is closed under intersection, which means that $\underline{\mathcal{W}}(\mathcal{L})$ contains a minimal subspace $\mathcal{W}^*\triangleq\inf\underline{\mathcal{W}}(\mathcal{L})$. In order to calculate $\mathcal{W}^*$, a recursive algorithm is proposed as shown below:

$$\begin{aligned}&\mathcal{W}_0=\mathcal{L},\\&\mathcal{W}_k=\mathcal{L}+\sum_{i=0}^{n_\rho}A_i(\mathcal{W}_{k-1}\cap\ker C)+\sum_{i=0}^{n_\rho}A_{\tau,i}(\mathcal{W}_{k-1}\cap\ker C).\end{aligned}$$

The above algorithm converges in finite steps, and the limit value is $\lim\mathcal{W}_k$. We have $\mathcal{W}^*=\lim\mathcal{W}_k$.

The notation $\underline{\mathcal{S}}(\mathcal{L})$ is employed to denote the set of $[C,\ A(\rho),\ A_\tau(\rho)]$-unobservability subspaces containing a subspace $\mathcal{L}\subseteq\mathcal{X}$. Similar to $\underline{\mathcal{W}}(\mathcal{L})$, $\underline{\mathcal{S}}(\mathcal{L})$ is also closed under intersection, which means that there is a minimum element $\mathcal{S}^*\triangleq\inf\underline{\mathcal{S}}(\mathcal{L})$. A recursive algorithm is proposed to calculate $\mathcal{S}^*$ as shown below:

$$\begin{aligned}&\mathcal{S}_0=\mathcal{X},\\&\mathcal{S}_k=\left[\mathcal{W}^*+\left(\bigcap_{i=0}^{n_\rho}(A_i^{-1}\mathcal{S}_{k-1})\right)\cap\ker C\right]\cap\left[\mathcal{W}^*+\left(\bigcap_{i=0}^{n_\rho}(A_{\tau,i}^{-1}\mathcal{S}_{k-1})\right)\cap\ker C\right].\end{aligned}$$

The given algorithm converges in finite steps, and the limit value is $\lim\mathcal{S}_k$. We have $\mathcal{S}^*=\lim\mathcal{S}_k$.

Remark 4. For brevity, the construction of the subspaces is not detailed here. For more details, refer to [30, 32–34].

4 H_∞-based geometric FDI observer

4.1 Observer design with exact-memory

In this subsection, we assume that the time delay $\tau(t)$ is precisely known. For each fault mode, we design a reduced-order observer as shown below to generate residual signals.

$$\begin{aligned}&\dot{w}_i(t)=N_i(\rho)w_i(t)+N_{i\tau}(\rho)w_i(t-\tau(t))-G_i(\rho)y(t)-G_{i\tau}(\rho)y(t-\tau(t))+F_i(\rho)u(t),\\&r_i(t)=M_iw_i(t)-H_iy(t),\\&w_i(\theta)=\phi_i(\theta),\ \theta\in[-\tau_M,\ 0],\end{aligned}\tag{8}$$

where w_i is the state of the observer and r_i is the residual signal. $N_i(\rho)$, $N_{i\tau}(\rho)$, $G_i(\rho)$, $G_{i\tau}(\rho)$, and $F_i(\rho)$ are the parameter matrices with affine form. M_i and H_i are constant matrices.

Let $e_i(t)=w_i(t)-P_{c_i}x(t)$, where P_{c_i} is a canonical projection. Now, we present a detailed description of the problem considered in this paper. The H_∞-based residual generation problem for the state time-delay LPV system (1) (marked as "HRGP-dLPV") is to construct a set of observers (8) to generate residuals that satisfy the following conditions.

(1) $m_i\mapsto r_j=0$, when $i\neq j$;

(2) $m_i\mapsto r_j$ is input observable, when $i=j$;

(3) when $m_i=0,\ d\neq0$, and the initial conditions are zero, the following inequality holds:

$$\|r_i\|_{L_2}<\gamma_i\|d\|_{L_2},\tag{9}$$

where γ_i is a scalar.

Remark 5. Conditions (1) and (2) of HRGP-dLPV mean that the output of i-th observer r_i is only sensitive to fault m_i and robust to all the other faults $m_j, j\neq i$.

The following lemmas are introduced to derive our main results.

Lemma 4 ([35])**.** Consider an integral quadratic term of the form

$$\ell_R(\omega)=\int_a^b\omega^{\mathrm{T}}(s)R\omega(s)\mathrm{d}s,$$

where $-\infty < a < b < +\infty$ are scalars, ω is a continuous function from $[a,b] \to \mathbb{R}^n$ and consequently integrable. With a given matrix $R \succ 0$, the following inequality holds for all continuously differentiable function ω in $[a,b] \to \mathbb{R}^n$:

$$\ell_R(\dot{\omega}) \geqslant \frac{1}{b-a}\left(\omega(b)-\omega(a)\right)^{\mathrm{T}} R\left(\omega(b)-\omega(a)\right) + \frac{3}{b-a}\Omega^{\mathrm{T}} R \Omega,$$

where $\Omega = \omega(b)+\omega(a)-\frac{2}{b-a}\int_a^b \omega(s)\mathrm{d}s$.

Lemma 5 ([36]). For given positive integers n, m, a scalar α in the interval $[0,\,1]$, a given $n\times n$-matrix $R \succ 0$, two matrices W_1 and W_2 in $\mathbb{R}^{n\times m}$, define, for all vector ξ in $\mathbb{R}^m$, the function $\Theta(\alpha, R)$ as

$$\Theta(\alpha,R) = \frac{1}{\alpha}\xi^{\mathrm{T}} W_1^{\mathrm{T}} R W_1 \xi + \frac{1}{1-\alpha}\xi^{\mathrm{T}} W_2^{\mathrm{T}} R W_2 \xi.$$

If there exists a matrix X in $\mathbb{R}^{n\times n}$ such that $\left[\begin{smallmatrix} R & X \\ * & R \end{smallmatrix}\right] \succ 0$, then the following inequality holds:

$$\min_{\alpha\in(0,1)} \Theta(\alpha,R) \geqslant \begin{bmatrix} W_1\xi \\ W_2\xi \end{bmatrix}^{\mathrm{T}} \begin{bmatrix} R & X \\ * & R \end{bmatrix} \begin{bmatrix} W_1\xi \\ W_2\xi \end{bmatrix}.$$

Remark 6. Lemma 4 is an inequality derived from Wirtinger's inequality, which is less conservative compared with Jensen's inequality [35].

According to the analysis of TPUS in Section 3, the geometric approach is introduced into time-delay LPV systems to separate different fault spaces. Based on this property, we can achieve fault detection and isolation simultaneously. Regarding system disturbances, we employ H_∞ techniques to suppress their effects. Considering the state time-delay LPV system (1) with $u(t)\equiv 0$ and $m_i(t)\equiv 0$, $\forall t \geqslant 0$, we have the following result.

Theorem 1. Assume that there exist $n\times n$-matrices $P\succ 0$, $S\succ 0$, $Q\succ 0$, $R\succ 0$, a $2n\times 2n$-matrix X, and a scalar $\gamma > 0$ such that the following matrix inequalities are satisfied for $\tau = \{\tau_m,\,\tau_M\}$ and $\dot{\tau} = \{\varsigma_m,\,\varsigma_M\}$:

$$\Phi_0(\tau,\dot{\tau}) = \Phi_1(\tau,\dot{\tau}) - \frac{1}{\tau_M}\Gamma^{\mathrm{T}}\Phi_2\Gamma - \Phi_3 \prec 0, \quad \Phi_2 = \begin{bmatrix} \tilde{R} & X \\ * & \tilde{R} \end{bmatrix} \succ 0, \tag{10}$$

where

$$\Phi_1(\tau,\dot{\tau}) = \mathrm{He}\left(G_1^{\mathrm{T}}(\tau)\hat{P}G_0(\dot{\tau})\right) + \hat{S} + \hat{Q}(\dot{\tau}) + \tau_M G_0^{\mathrm{T}}(\dot{\tau})\hat{R}G_0(\dot{\tau}),\ \Gamma = \begin{bmatrix} G_2^{\mathrm{T}} & G_3^{\mathrm{T}} & G_4^{\mathrm{T}} & G_5^{\mathrm{T}} \end{bmatrix}^{\mathrm{T}},$$

$$\Phi_3 = \begin{bmatrix} -C^{\mathrm{T}}C & 0\ 0\ 0\ 0 & -C^{\mathrm{T}}D^d \\ * & 0\ 0\ 0\ 0 & 0 \\ * & *\ 0\ 0\ 0 & 0 \\ * & *\ *\ 0\ 0 & 0 \\ * & *\ *\ *\ 0 & 0 \\ * & *\ *\ *\ *\ * & \gamma^2 I - (D^d)^{\mathrm{T}}D^d \end{bmatrix},$$

$$G_2 = \begin{bmatrix} I & -I & 0 & 0 & 0 & 0 \end{bmatrix},\ G_3 = \begin{bmatrix} I & I & 0 & -2I & 0 & 0 \end{bmatrix},\ G_4 = \begin{bmatrix} 0 & I & -I & 0 & 0 & 0 \end{bmatrix},\ G_5 = \begin{bmatrix} 0 & I & I & 0 & -2I & 0 \end{bmatrix},$$

$$\hat{P} = \mathrm{diag}(P,P,P),\ \hat{Q}(\dot{\tau}) = \mathrm{diag}(Q, -(1-\dot{\tau})Q, 0_{4n}),$$

$$\hat{S} = \mathrm{diag}(S, 0, -S, 0_{3n}),\ \hat{R} = \mathrm{diag}(R, 0_{2n}),\ \tilde{R} = \mathrm{diag}(R, 3R),$$

$$G_0(\dot{\tau}) = \begin{bmatrix} A(\rho) & A_\tau(\rho) & 0 & 0\ 0 & B^d(\rho) \\ I & -(1-\dot{\tau})I & 0 & 0\ 0 & 0 \\ 0 & (1-\dot{\tau})I & -I & 0\ 0 & 0 \end{bmatrix},\ G_1(\tau) = \begin{bmatrix} I & 0\ 0 & 0 & 0 & 0 \\ 0 & 0\ 0 & \tau I & 0 & 0 \\ 0 & 0\ 0 & 0 & (\tau_M-\tau)I & 0 \end{bmatrix}.$$

Then the system (1) with $u(t)\equiv 0$ and $m_i(t)\equiv 0$ satisfies $\|y\|_{L_2} < \gamma\|d\|_{L_2}$.

Proof. Consider the Lyapunov-Krasovskii functional as follows:

$$V = \tilde{x}^{\mathrm{T}}(t)\hat{P}\tilde{x}(t) + \int_{t-\tau(t)}^{t} x^{\mathrm{T}}(\eta)Qx(\eta)\mathrm{d}\eta + \int_{t-\tau_M}^{t} x^{\mathrm{T}}(\eta)Sx(\eta)\mathrm{d}\eta + \int_{t-\tau_M}^{t}\int_{\theta}^{t} \dot{x}^{\mathrm{T}}(\eta)R\dot{x}(\eta)\mathrm{d}\eta\mathrm{d}\theta,$$

where $\tilde{x}(t) \triangleq [x^{\mathrm{T}}(t), \int_{t-\tau(t)}^{t} x^{\mathrm{T}}(\eta)\mathrm{d}\eta, \int_{t-\tau_M}^{t-\tau(t)} x^{\mathrm{T}}(\eta)\mathrm{d}\eta]^{\mathrm{T}}$.

The derivative of the function along the trajectory of (1) leads to

$$\begin{aligned}\dot{V} = {} & \dot{\tilde{x}}^{\mathrm{T}}(t)\hat{P}\tilde{x}(t) + \tilde{x}^{\mathrm{T}}(t)\hat{P}\dot{\tilde{x}}(t) + x^{\mathrm{T}}(t)Qx(t) - (1-\dot{\tau}(t))x^{\mathrm{T}}(t-\tau(t))Qx(t-\tau(t)) \\ & + x^{\mathrm{T}}(t)Sx(t) - x^{\mathrm{T}}(t-\tau_M)Sx(t-\tau_M) + \tau_M\dot{x}^{\mathrm{T}}(t)R\dot{x}(t) - \int_{t-\tau_M}^{t} \dot{x}^{\mathrm{T}}(\eta)R\dot{x}(\eta)\mathrm{d}\eta.\end{aligned} \tag{11}$$

Let

$$\zeta_1^{\mathrm{T}}(t) = \left[x^{\mathrm{T}}(t),\ x^{\mathrm{T}}(t-\tau(t)),\ x^{\mathrm{T}}(t-\tau_M),\ \frac{1}{\tau(t)}\int_{t-\tau(t)}^{t} x^{\mathrm{T}}(\eta)\mathrm{d}\eta,\ \frac{1}{\tau_M-\tau(t)}\int_{t-\tau_M}^{t-\tau(t)} x^{\mathrm{T}}(\eta)\mathrm{d}\eta,\ d^{\mathrm{T}}(t)\right].$$

We have $\tilde{x}(t) = G_1(\tau)\zeta_1(t)$ and $\dot{\tilde{x}}(t) = G_0(\dot{\tau})\zeta_1(t)$.

Next, we divide the integral term into two intervals $[t-\tau_M,\, t-\tau(t)]$ and $[t-\tau(t),\, t]$, and integrate them respectively. Using Lemma 4, we can get

$$\int_{t-\tau_M}^{t} \dot{x}^{\mathrm{T}}(s)R\dot{x}(s)\mathrm{d}s \geqslant \zeta_1^{\mathrm{T}}(t)\left(\frac{1}{\tau(t)}G_{2,3}^{\mathrm{T}}\tilde{R}G_{2,3} + \frac{1}{\tau_M-\tau(t)}G_{4,5}^{\mathrm{T}}\tilde{R}G_{4,5}\right)\zeta_1(t),$$

where $G_{2,3} = [G_2^{\mathrm{T}}\ G_3^{\mathrm{T}}]^{\mathrm{T}}$ and $G_{4,5} = [G_4^{\mathrm{T}}\ G_5^{\mathrm{T}}]^{\mathrm{T}}$. Based on Lemma 5, if there exists a matrix X such that $\Phi_2 = \left[\begin{smallmatrix}\tilde{R} & X\\ * & \tilde{R}\end{smallmatrix}\right] \succ 0$, we can draw that

$$\int_{t-\tau_M}^{t} \dot{x}^{\mathrm{T}}(s)R\dot{x}(s)\mathrm{d}s \geqslant \frac{1}{\tau_M}\zeta_1^{\mathrm{T}}(t)\Gamma^{\mathrm{T}}\Phi_2\Gamma\zeta_1(t).$$

With the system output equation $y(t) = Cx(t) + D^d d(t)$, we can deduce that

$$\gamma^2 d^{\mathrm{T}}(t)d(t) - y^{\mathrm{T}}(t)y(t) = \zeta_1^{\mathrm{T}}(t)\Phi_3\zeta_1(t). \tag{12}$$

According to (11) and (12), it shows

$$\dot{V} - \gamma^2 d^{\mathrm{T}}(t)d(t) + y^{\mathrm{T}}(t)y(t) \leqslant \zeta_1^{\mathrm{T}}(t)\Phi_0\zeta_1(t).$$

Therefore,

$$\dot{V} - \gamma^2 d^{\mathrm{T}}(t)d(t) + y^{\mathrm{T}}(t)y(t) \prec 0 \tag{13}$$

holds if there exists a matrix X such that $\Phi_2 \succ 0$ and if $\Phi_0 \prec 0$, for all $(\tau, \dot{\tau}) \in [\tau_m, \tau_M] \times [\varsigma_m, \varsigma_M]$. Since the matrix Φ_0 is affine, and consequently convex, with respect to $\tau(t)$ and $\dot{\tau}(t)$, it is necessary and sufficient to ensure that $\Phi_0 \prec 0$ at the vertices of the intervals $[\tau_m,\, \tau_M] \times [\varsigma_m,\, \varsigma_M]$.

Under zero initial conditions, integrating both sides of (13) yields $\|y\|_{L_2} < \gamma\|d\|_{L_2}$. Consequently, the H_∞ performance is guaranteed. This concludes the proof.

Based on Theorem 1, the main result in this subsection is proposed.

Theorem 2. Under the assumption that the time delay $\tau(t)$ is precisely known, the HRGP-dLPV problem has a solution if there exist $[C,\, A(\rho),\, A_\tau(\rho)]$-unobservability subspaces $\mathcal{S}_i^*$ such that

$$\mathcal{L}_i \cap \mathcal{S}_i^* = 0,\ i \in \boldsymbol{k},\ \forall \rho \in \mathcal{P}, \tag{14}$$

where $\mathcal{S}_i^* = \inf \underline{\mathcal{S}}(\sum_{j=1,j\neq i}^{k} \mathcal{L}_j)$, and there exist $n \times n$-matrices $P_i \succ 0$, $S_i \succ 0$, $Q_i \succ 0$, $R_i \succ 0$, $X_{i_{11}}$, $X_{i_{12}}$, $X_{i_{21}}$, $X_{i_{22}}$, continuously differentiable matrix functions $T_{i_{p1}}(\rho)$, $T_{i_{p2}}(\rho)$, $T_{i_{r1}}(\rho)$, $T_{i_{r2}}(\rho)$, and scalars

$\gamma_i > 0$ such that the following matrix inequalities are satisfied for $\tau = \{\tau_m, \tau_M\}$ and $\dot{\tau} = \{\varsigma_m, \varsigma_M\}$:

$$\Psi_{i_0}(\tau,\dot{\tau}) = \begin{bmatrix} \psi_{i_{11}} & \psi_{i_{12}} & \psi_{i_{13}} & \psi_{i_{14}} & \psi_{i_{15}} & \psi_{i_{16}} & \psi_{i_{17}} \\ * & \psi_{i_{22}} & \psi_{i_{23}} & \psi_{i_{24}} & \psi_{i_{25}} & 0 & \psi_{i_{27}} \\ * & * & \psi_{i_{33}} & \psi_{i_{34}} & \psi_{i_{35}} & 0 & 0 \\ * & * & * & \psi_{i_{44}} & \psi_{i_{45}} & 0 & 0 \\ * & * & * & * & \psi_{i_{55}} & 0 & 0 \\ * & * & * & * & * & \psi_{i_{66}} & \psi_{i_{67}} \\ * & * & * & * & * & * & \psi_{i_{77}} \end{bmatrix} \prec 0, \quad \Psi_{i_1} = \begin{bmatrix} \tilde{R}_i & X_i \\ * & \tilde{R}_i \end{bmatrix} \succ 0, \tag{15}$$

where

$$\begin{aligned}
&\psi_{i_{11}} = \mathrm{He}\{P_i A_{i_0}(\rho) + T_{i_{p1}}(\rho) M_i\} + S_i + Q_i - \frac{4}{\tau_M} R_i + M_i^{\mathrm{T}} M_i,\\
&\psi_{i_{12}} = P_i A_{i_{\tau,0}}(\rho) + T_{i_{p2}}(\rho) M_i - \frac{1}{\tau_M}(2R + X_{i_{11}} + X_{i_{12}} + X_{i_{21}} + X_{i_{22}}),\\
&\psi_{i_{13}} = -\frac{1}{\tau_M}(-X_{i_{11}} - X_{i_{21}} + X_{i_{12}} + X_{i_{22}}), \quad \psi_{i_{14}} = \tau P_i + \frac{6}{\tau_M} R_i, \quad \psi_{i_{15}} = \frac{2}{\tau_M}(X_{i_{12}} + X_{i_{22}}),\\
&\psi_{i_{16}} = \begin{bmatrix} \epsilon_{i_1} & \epsilon_{i_2} \end{bmatrix}, \quad \epsilon_{i_1} = -P_i P_{c_i} D_{i_0}(\rho) D^d - T_{i_{p1}}(\rho) H_i D^d - P_i P_{c_i} B^d(\rho) + M_i^{\mathrm{T}} H_i D^d,\\
&\epsilon_{i_2} = -P_i P_{c_i} D_{i_{\tau,0}}(\rho) D^d - T_{i_{p2}}(\rho) H_i D^d, \quad \psi_{i_{17}} = A_{i_0}^{\mathrm{T}}(\rho) R_i + M_i^{\mathrm{T}} T_{i_{r1}}(\rho),\\
&\psi_{i_{22}} = -(1-\dot{\tau}) Q_i - \frac{1}{\tau_M}(8R_i - X_{i_{11}} - X_{i_{11}}^{\mathrm{T}} - X_{i_{12}} - X_{i_{12}}^{\mathrm{T}} + X_{i_{21}} + X_{i_{21}}^{\mathrm{T}} + X_{i_{22}} + X_{i_{22}}^{\mathrm{T}}),\\
&\psi_{i_{23}} = -\frac{1}{\tau_M}(2R_i + X_{i_{11}} - X_{i_{21}} - X_{i_{12}} + X_{i_{22}}), \quad \psi_{i_{24}} = -\tau(1-\dot{\tau}) P_i + \frac{2}{\tau_M}(3R_i + X_{i_{21}}^{\mathrm{T}} + X_{i_{22}}^{\mathrm{T}}),\\
&\psi_{i_{25}} = (1-\dot{\tau})(\tau_M - \tau) P_i + \frac{2}{\tau_M}(3R_i - X_{i_{12}} + X_{i_{22}}), \quad \psi_{i_{27}} = A_{i_{\tau,0}}^{\mathrm{T}}(\rho) R_i + M_i^{\mathrm{T}} T_{i_{r2}}(\rho),\\
&\psi_{i_{33}} = -S_i - \frac{4}{\tau_M} R_i, \quad \psi_{i_{34}} = \frac{2}{\tau_M}(-X_{i_{21}}^{\mathrm{T}} + X_{i_{22}}^{\mathrm{T}}), \quad \psi_{i_{35}} = -(\tau_M - \tau) P_i + \frac{6}{\tau_M} R_i,\\
&\psi_{i_{44}} = \psi_{i_{55}} = -\frac{12}{\tau_M} R_i, \quad \psi_{i_{45}} = -\frac{4}{\tau_M} X_{i_{22}}, \quad \psi_{i_{77}} = -\frac{1}{\tau_M} R_i,\\
&\psi_{i_{66}} = -\gamma_i^2 I + \begin{bmatrix} (D^d)^{\mathrm{T}} H_i^{\mathrm{T}} H_i D^d & 0 \\ 0 & 0 \end{bmatrix}, \quad \psi_{i_{67}} = \begin{bmatrix} \epsilon_{i_3} \\ \epsilon_{i_4} \end{bmatrix}, \quad X_i = \begin{bmatrix} X_{i_{11}} & X_{i_{12}} \\ X_{i_{21}} & X_{i_{22}} \end{bmatrix}, \quad \tilde{R}_i = \mathrm{diag}(R_i, 3R_i),\\
&\epsilon_{i_3} = -(D^d)^{\mathrm{T}} D_{i_0}^{\mathrm{T}}(\rho) P_{c_i}^{\mathrm{T}} R_i - (D^d)^{\mathrm{T}} H_i^{\mathrm{T}} T_{i_{r1}}(\rho) - (B^d(\rho))^{\mathrm{T}} P_{c_i}^{\mathrm{T}} R_i,\\
&\epsilon_{i_4} = -(D^d)^{\mathrm{T}} D_{i_{\tau,0}}^{\mathrm{T}}(\rho) P_{c_i}^{\mathrm{T}} R_i - (D^d)^{\mathrm{T}} H_i^{\mathrm{T}} T_{i_{r2}}(\rho),
\end{aligned}$$

P_{c_i} is the canonical projection of $\mathcal{X}$ on $\mathcal{X}/\mathcal{S}_i^*$, $D_{i_0}(\rho)$ is a map satisfying $(A(\rho)+D_{i_0}(\rho)C)\mathcal{S}_i^* \subseteq \mathcal{S}_i^*$, $A_{i_0}(\rho)$ is a map induced by $A(\rho)+D_{i_0}(\rho)C$ on $\mathcal{X}/\mathcal{S}_i^*$, $D_{i_{\tau,0}}(\rho)$ is a map satisfying $(A_\tau(\rho)+D_{i_{\tau,0}}(\rho)C)\mathcal{S}_i^* \subseteq \mathcal{S}_i^*$, $A_{i_{\tau,0}}(\rho)$ is a map induced by $A_\tau(\rho)+D_{i_{\tau,0}}(\rho)C$ on $\mathcal{X}/\mathcal{S}_i^*$, H_i is calculated by $\ker H_i C = \mathcal{S}_i^* + \ker C$, and M_i is given by $M_i P_{c_i} = H_i C$.

Proof. If the unobservability subspaces satisfy (14), then according to the geometric approach, a set of observers satisfying conditions (1) and (2) exists. Through solving matrix inequalities (15), we get $T_{i_{p1}}(\rho)$ and $T_{i_{p2}}(\rho)$. Let $D_{i_1}(\rho) = P_i^{-1} T_{i_{p1}}(\rho)$, $D_{i_{\tau,1}}(\rho) = P_i^{-1} T_{i_{p2}}(\rho)$, and define $N_i(\rho) = A_{i_0}(\rho) + D_{i_1}(\rho) M_i$, $N_{i\tau}(\rho) = A_{i_{\tau,0}}(\rho) + D_{i_{\tau,1}}(\rho) M_i$, $G_i(\rho) = P_{c_i}(D_{i_0}(\rho) + P_{c_i}^{-r} D_{i_1}(\rho) H_i)$, $G_{i\tau}(\rho) = P_{c_i}(D_{i_{\tau,0}}(\rho) + P_{c_i}^{-r} D_{i_{\tau,1}}(\rho) H_i)$, and $F_i(\rho) = P_{c_i} B(\rho)$. Therefore, we get the parameters of the observers. According to $e_i = w_i - P_{c_i} x$, we get

$$\begin{aligned}
\dot{e}_i(t) &= N_i(\rho) w_i(t) + N_{i\tau}(\rho) w_i(t-\tau(t)) - P_{c_i}(D_{i_0}(\rho) + P_{c_i}^{-r} D_{i_1}(\rho) H_i)(Cx(t) + D^d d(t))\\
&\quad - P_{c_i}(D_{i_{\tau,0}}(\rho) + P_{c_i}^{-r} D_{i_{\tau,1}}(\rho) H_i)(Cx(t-\tau(t)) + D^d d(t-\tau(t))) - P_{c_i} A(\rho) x(t)\\
&\quad - P_{c_i} A_\tau(\rho) x(t-\tau(t)) - P_{c_i} L_i(\rho) m_i(t) - P_{c_i} B^d(\rho) d(t)\\
&= N_i(\rho) w_i(t) + N_{i\tau}(\rho) w_i(t-\tau(t)) - P_{c_i}(A(\rho) + D_{i_0}(\rho) C) x(t) - P_{c_i}(A_\tau(\rho)\\
&\quad + D_{i_{\tau,0}}(\rho) C) x(t-\tau(t)) - D_{i_1}(\rho) M_i P_{c_i} x(t) - D_{i_{\tau,1}}(\rho) M_i P_{c_i} x(t-\tau(t))
\end{aligned}$$

$$
\begin{aligned}
&- \epsilon_{i_5} d(t) - \epsilon_{i_6} d(t-\tau(t)) - P_{c_i} L_i(\rho) m_i(t) \\
&= (A_{i_0}(\rho) + D_{i_1}(\rho) M_i) e(t) + (A_{i_{\tau,0}}(\rho) + D_{i_{\tau,1}}(\rho) M_i) e(t-\tau(t)) - P_{c_i} L_i(\rho) m_i(t) \\
&\quad - \begin{bmatrix} \epsilon_{i_5} & \epsilon_{i_6} \end{bmatrix} \begin{bmatrix} d(t) \\ d(t-\tau(t)) \end{bmatrix}, \\
r_i(t) &= M_i w_i(t) - H_i C x(t) - H_i D^d d(t) = M_i e(t) - H_i \begin{bmatrix} D^d & 0 \end{bmatrix} \begin{bmatrix} d(t) \\ d(t-\tau(t)) \end{bmatrix},
\end{aligned}
$$

where $\epsilon_{i_5} = P_{c_i} D_{i_0}(\rho) D^d + D_{i_1}(\rho) H_i D^d + P_{c_i} B^d(\rho)$, $\epsilon_{i_6} = P_{c_i} D_{i_{\tau,0}}(\rho) D^d + D_{i_{\tau,1}}(\rho) H_i D^d$. Based on Theorem 1, we can get a set of matrix inequalities, which contains the quadratic product term of some unknown matrices. Using Schur complements to perform an equivalent transformation, we can draw matrix inequalities (15), which concludes the proof.

4.2 Observer design with rough-memory

Different from Subsection 4.1, we assume that the time delay $\tau(t)$ is not known precisely, and we can only get an estimated value $\tilde{\tau}(t)$ in this part. Without loss of generality, we set $\tilde{\tau}(t)$ to meet constraints (2), that is, $\tilde{\tau}(t) \in [\tau_m, \tau_M]$, $\dot{\tilde{\tau}}(t) \in [\varsigma_m, \varsigma_M]$, $\forall t \geqslant 0$. We assume that $|\tilde{\tau}(t) - \tau(t)| \leqslant \varrho$ for some $\varrho > 0$, and the error signal $\hat{x}(t) \triangleq x(t-\tilde{\tau}(t)) - x(t-\tau(t))$ is L_2-norm bounded.

For each fault mode, we design the reduced-order observer as shown below to generate residuals:

$$
\begin{aligned}
&\dot{w}_i(t) = N_i(\rho) w_i(t) + N_{i\tau}(\rho) w_i(t-\tilde{\tau}(t)) - G_i(\rho) y(t) - G_{i\tau}(\rho) y(t-\tilde{\tau}(t)) + F_i(\rho) u(t), \\
&r_i(t) = M_i w_i(t) - H_i y(t), \\
&w_i(\theta) = \phi_i(\theta),\ \theta \in [-\tau_M, 0].
\end{aligned} \tag{16}
$$

Similarly, we can draw the following conclusion.

Theorem 3. Under the assumption that the time delay $\tau(t)$ is not known precisely, and only an estimated value can be obtained, the HRGP-dLPV problem has a solution if there exist $[C, A(\rho), A_\tau(\rho)]$-unobservability subspaces $\mathcal{S}_i^*$ such that

$$
\mathcal{L}_i(\rho) \cap \mathcal{S}_i^* = 0,\ i \in \boldsymbol{k},\ \forall \rho \in \mathcal{P}, \tag{17}
$$

where $\mathcal{S}_i^* = \inf \underline{\mathcal{S}}(\sum_{j=1, j\neq i}^{k} \mathcal{L}_j)$, and there exist $n \times n$-matrices $P_i \succ 0$, $S_i \succ 0$, $Q_i \succ 0$, $R_i \succ 0$, $X_{i_{11}}$, $X_{i_{12}}$, $X_{i_{21}}$, $X_{i_{22}}$, continuously differentiable matrix functions $T_{i_{p1}}(\rho)$, $T_{i_{p2}}(\rho)$, $T_{i_{r1}}(\rho)$, $T_{i_{r2}}(\rho)$, and scalars $\gamma_i > 0$ such that the following matrix inequalities are satisfied for $\tilde{\tau} = \{\tau_m, \tau_M\}$ and $\dot{\tilde{\tau}} = \{\varsigma_m, \varsigma_M\}$:

$$
\Psi_{i_0}(\tilde{\tau}, \dot{\tilde{\tau}}) = \begin{bmatrix}
\psi_{i_{11}} & \psi_{i_{12}} & \psi_{i_{13}} & \psi_{i_{14}} & \psi_{i_{15}} & \psi_{i_{16}} & \psi_{i_{17}} \\
* & \psi_{i_{22}} & \psi_{i_{23}} & \psi_{i_{24}} & \psi_{i_{25}} & 0 & \psi_{i_{27}} \\
* & * & \psi_{i_{33}} & \psi_{i_{34}} & \psi_{i_{35}} & 0 & 0 \\
* & * & * & \psi_{i_{44}} & \psi_{i_{45}} & 0 & 0 \\
* & * & * & * & \psi_{i_{55}} & 0 & 0 \\
* & * & * & * & * & \psi_{i_{66}} & \psi_{i_{67}} \\
* & * & * & * & * & * & \psi_{i_{77}}
\end{bmatrix} \prec 0, \quad \Psi_{i_1} = \begin{bmatrix} \tilde{R}_i & X_i \\ * & \tilde{R}_i \end{bmatrix} \succ 0, \tag{18}
$$

where

$$
\begin{aligned}
&\psi_{i_{16}} = \begin{bmatrix} \epsilon_{i_1} & \epsilon_{i_2} & \epsilon_{i_3} \end{bmatrix}, \quad \epsilon_{i_1} = -P_i P_{c_i} D_{i_0}(\rho) D^d - T_{i_{p1}}(\rho) H_i D^d - P_i P_{c_i} B^d(\rho) + M_i^{\mathrm{T}} H_i D^d, \\
&\epsilon_{i_2} = -P_i P_{c_i} D_{i_{\tau,0}}(\rho) D^d - T_{i_{p2}}(\rho) H_i D^d, \quad \epsilon_{i_3} = P_i P_{c_i} A_\tau(\rho), \\
&\psi_{i_{66}} = -\gamma_i^2 I + \begin{bmatrix} (D^d)^{\mathrm{T}} H_i^{\mathrm{T}} H_i D^d & 0 & 0 \\ 0 & 0 & 0 \\ 0 & 0 & 0 \end{bmatrix}, \quad \psi_{i_{67}} = \begin{bmatrix} \epsilon_{i_4} \\ \epsilon_{i_5} \\ \epsilon_{i_6} \end{bmatrix}, \\
&\epsilon_{i_4} = -(D^d)^{\mathrm{T}} D_{i_0}^{\mathrm{T}}(\rho) P_{c_i}^{\mathrm{T}} R_i - (D^d)^{\mathrm{T}} H_i^{\mathrm{T}} T_{i_{r1}}(\rho) - (B^d(\rho))^{\mathrm{T}} P_{c_i}^{\mathrm{T}} R_i,
\end{aligned}
$$

$$\epsilon_{i_5} = -(D^d)^{\mathrm{T}} D_{i_{\tau,0}}^{\mathrm{T}}(\rho) P_{c_i}^{\mathrm{T}} R_i - (D^d)^{\mathrm{T}} H_i^{\mathrm{T}} T_{i_{r2}}(\rho), \quad \epsilon_{i_6} = A_\tau^{\mathrm{T}}(\rho) P_{c_i}^{\mathrm{T}} R_i,$$

and other sub-matrices are the same as defined in Theorem 2 by replacing $\tau(t)$ with $\tilde{\tau}(t)$.

Proof. Similar to the proof of Theorem 2, by solving matrix inequality (18), we can obtain the observer parameters $N_i(\rho)$, $N_{i\tau}(\rho)$, $G_i(\rho)$, $G_{i\tau}(\rho)$ and $F_i(\rho)$. Therefore, we get

$$\dot{e}_i(t) = (A_{i_0}(\rho) + D_{i_1}(\rho)M_i)e(t) + (A_{i_{\tau,0}}(\rho) + D_{i_{\tau,1}}(\rho)M_i)e(t-\tilde{\tau}(t)) - P_{c_i}L_i(\rho)m_i(t) - \begin{bmatrix}\epsilon_{i_7} & \epsilon_{i_8} & \epsilon_{i_9}\end{bmatrix}\hat{d}(t),$$
$$r_i(t) = M_i e(t) - H_i \begin{bmatrix}D^d & 0 & 0\end{bmatrix}\hat{d}(t),$$

where $\epsilon_{i_7} = P_{c_i}D_{i_0}(\rho)D^d + D_{i_1}(\rho)H_iD^d + P_{c_i}B^d(\rho)$, $\epsilon_{i_8} = P_{c_i}D_{i_{\tau,0}}(\rho)D^d + D_{i_{\tau,1}}(\rho)H_iD^d$, $\epsilon_{i_9} = -P_{c_i}A_\tau(\rho)$, and $\hat{d}(t) = [d(t)\ d(t-\tilde{\tau}(t))\ \hat{x}(t)]^{\mathrm{T}}$. Similarly, based on Theorem 1 and Schur complements, we can draw matrix inequalities (18), which concludes the proof.

Remark 7. A series of results have been proposed to estimate the time delay of the system, for example, expectation-maximization algorithm [37], maximum likelihood optimization approach [38], adaptive identification technique [39], neural networks [40], and Bayesian-based approach [22]. An appropriate algorithm can be selected through experiments to get an estimation of the time delay, which is not discussed in detail in this article.

Remark 8. The matrix inequalities in Theorems 1–3 are all parameter-dependent matrix inequalities, and all the parameter-dependent matrices are affine functions of the time-varying parameters. In this work, the gridding techniques in [23] are utilized to solve these matrix inequalities.

4.3 Residual evaluation

According to HRGP-dLPV conditions (1) and (2), r_i is only affected by fault m_i and has successfully been decoupled from all the other faults m_j, $j \neq i$. Accordingly, fault detection and fault isolation can be completed at the same time. In this subsection, the design of the evaluation function for residual signals is detailed. We choose the following residual evaluation function:

$$J_i(t) = \frac{1}{T_r}\left(\int_{t-T_r}^{t} r_i^{\mathrm{T}}(\eta) r_i(\eta) \mathrm{d}\eta\right)^{\frac{1}{2}}, \tag{19}$$

where T_r is the length of the evaluation time window. Subsequently, the threshold is selected as follows:

$$J_i^{\mathrm{th}} = \sup_{m_i=0} J_i(t). \tag{20}$$

Based on the above evaluation functions and thresholds, the occurrence of a fault can be alarmed through the following decision rules:

$$\begin{aligned} &J_i(t) > J_i^{\mathrm{th}} \Rightarrow \text{fault } m_i \text{ occurs}, i \in \boldsymbol{k}, \\ &J_i(t) \leqslant J_i^{\mathrm{th}} \Rightarrow \text{fault } m_i \text{ dose not occur}, i \in \boldsymbol{k}. \end{aligned} \tag{21}$$

Remark 9. It should be pointed out that Eq. (20) is a theoretical guidance for selecting the threshold. When taking into account an actual experiment, Eq. (20) is not appropriate to determine the threshold. This is because the assumption that $d(t)$ is L_2-norm bounded is a very constrained condition, and it is challenging to determine the precise value of the threshold. In practice, the threshold can be established using experiments or Monte Carlo simulations, and manually adjusted to compromise the missing alarm and the false alarm.

5 Numerical simulation

5.1 Case study I

In this subsection, we apply the proposed scheme to a widely used numerical model quoted from [41] to demonstrate the effectiveness of the strategy. The system model is shown as follows:

$$\begin{aligned}\dot{x}(t) =& \begin{bmatrix} 0 & 1+0.2\rho \\ -2 & -3+0.1\rho \end{bmatrix} x(t) + \begin{bmatrix} 0.2\rho & 0.1 \\ -0.2+0.1\rho & -0.3 \end{bmatrix} x(t-\tau(t)) + \begin{bmatrix} 0.2\rho \\ 0.1+0.1\rho \end{bmatrix} u(t) \\ &+ \begin{bmatrix} 0.2 \\ 0.2 \end{bmatrix} d(t) + \begin{bmatrix} 0 \\ 0.1 \end{bmatrix} m_1(t) + \begin{bmatrix} 0.2 \\ 0 \end{bmatrix} m_2(t), \\ y(t) =& \begin{bmatrix} 0 & 10 \\ 10 & 0 \end{bmatrix} x(t) + \begin{bmatrix} 0.1 \\ 0.1 \end{bmatrix} d(t),\end{aligned}$$

where $\rho = \sin(t)$, $\tau_m = 0$, $\tau_M = 0.5$, $\varsigma_m = -0.5$, and $\varsigma_M = 0.5$. The system disturbance is set to $d(t) = 2\sin(10t)\delta(t)$ during the simulation period, where $\delta(t) \in [-0.5, 0.5]$ is a uniformly distributed random variable. The initial states are set as $x(t) = [1,\ 1]^{\mathrm{T}}, \forall t \in [-0.5,\ 0]$. The state feedback controller in [42] is utilized to control the system. In this simulation, we consider that there are two faults, and the fault signals are set to

$$m_1(t) = \begin{cases} 2, & 20\,\mathrm{s} < t \leqslant 40\,\mathrm{s}, \\ 0, & \text{otherwise}, \end{cases} \quad m_2(t) = \begin{cases} 1, & 25\,\mathrm{s} < t \leqslant 45\,\mathrm{s}, \\ 0, & \text{otherwise}. \end{cases}$$

It can be seen that two faults exist simultaneously between 25–40 s.

5.1.1 *Exact-memory FDI observer*

We consider that the time-delay is exactly known and apply Theorem 2 to calculate the observer matrices. Verifying the matrix inequalities (15) over a grid of 65 points yields the matrices as follows:

$$\begin{aligned}&N_1(\rho) = -\,21.9821 + 0.1\rho,\ N_{1\tau}(\rho) = -0.3493 + 0.0653\rho,\ F_1(\rho) = -0.1 - 0.1\rho,\ M_1 = -1,\ H_1 = \begin{bmatrix} 0.1 & 0 \end{bmatrix}, \\ &G_1(\rho) = \begin{bmatrix} 1.8982 & -0.2 \end{bmatrix} + \begin{bmatrix} 7.1304 \times 10^{-7} & 0 \end{bmatrix} \rho,\ G_{1\tau}(\rho) = \begin{bmatrix} 0.0049 & -0.02 \end{bmatrix} + \begin{bmatrix} -0.0065 & 0.01 \end{bmatrix} \rho, \\ &N_2(\rho) = -\,17.2017 + 0.2\rho,\ N_{2\tau}(\rho) = 0.0446 + 0.1456\rho,\ F_2(\rho) = 0.2\rho,\ M_2 = 1,\ H_2 = \begin{bmatrix} 0 & 0.1 \end{bmatrix}, \\ &G_2(\rho) = \begin{bmatrix} -0.1 & -1.7202 \end{bmatrix} + \begin{bmatrix} -0.02 & 0.02 \end{bmatrix} \rho,\ G_{2\tau}(\rho) = \begin{bmatrix} -0.01 & 0.0045 \end{bmatrix} + \begin{bmatrix} 0 & -0.0054 \end{bmatrix} \rho.\end{aligned}$$

We set the length of the evaluation window as $T_r = 0.5$ s, and the thresholds are selected as $J_1^{\mathrm{th}} = J_2^{\mathrm{th}} = 0.8 \times 10^{-3}$. The evaluation function when two faults occur simultaneously is presented in Figure 1. As can be seen in the figure, the evaluation function $J_1(t)\,(J_2(t))$ is only affected by the single fault $m_1(t)\,(m_2(t))$ and not by the other fault $m_2(t)\,(m_1(t))$, which illustrates that the proposed method can effectively detect and isolate faults in state time-delay LPV systems.

5.1.2 *Rough-memory FDI observer*

In this part, we consider that the time-delay is unknown, and we can get an estimated value. We set $\varrho = \frac{\tau_M - \tau_m}{2}$. Same as the previous part, verifying the matrix inequalities (18) of Theorem 3 over a grid of 65 points yields the observer parameter matrices as follows:

$$\begin{aligned}&N_1(\rho) = -\,45.7239 + 2.6884\rho,\ N_{1\tau}(\rho) = -0.2017 + 0.0213\rho,\ F_1(\rho) = -0.1 - 0.1\rho,\ M_1 = -1, \\ &G_1(\rho) = \begin{bmatrix} 4.2724 & -0.2 \end{bmatrix} + \begin{bmatrix} -0.2588 & 0 \end{bmatrix} \rho,\ G_{1\tau}(\rho) = \begin{bmatrix} -0.0098 & -0.02 \end{bmatrix} + \begin{bmatrix} 0.0021 & 0.01 \end{bmatrix} \rho,\ H_1 = \begin{bmatrix} 0.1 & 0 \end{bmatrix}, \\ &N_2(\rho) = -\,19.7607 + 0.0355\rho,\ N_{2\tau}(\rho) = -0.2505 + 0.0125\rho,\ F_2(\rho) = 0.2\rho,\ M_2 = 1,\ H_2 = \begin{bmatrix} 0 & 0.1 \end{bmatrix}, \\ &G_2(\rho) = \begin{bmatrix} -0.1 & -1.9761 \end{bmatrix} + \begin{bmatrix} -0.02 & 0.0035 \end{bmatrix} \rho,\ G_{2\tau}(\rho) = \begin{bmatrix} -0.01 & -0.0251 \end{bmatrix} + \begin{bmatrix} 0 & -0.0187 \end{bmatrix} \rho.\end{aligned}$$

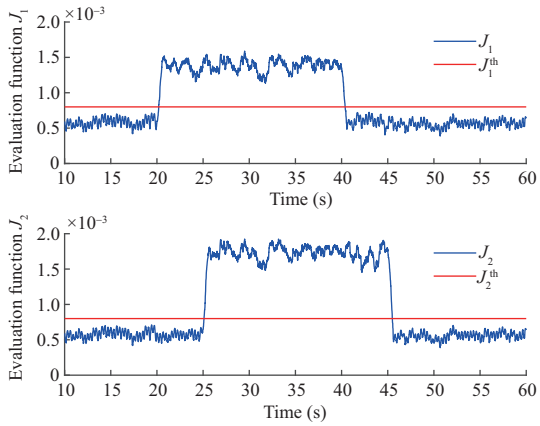

Figure 1 (Color online) Case study I: evaluation function with exact-memory when faults m_1 and m_2 occur simultaneously.

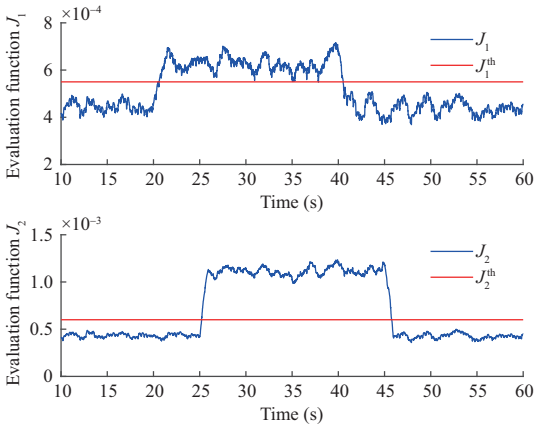

Figure 2 (Color online) Case study I: evaluation function with rough-memory when faults m_1 and m_2 occur simultaneously.

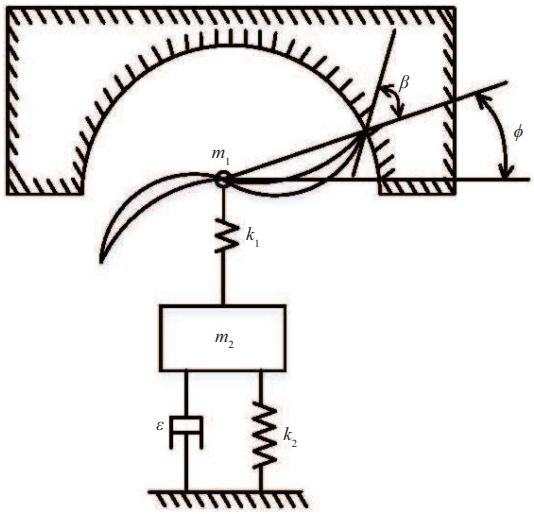

Figure 3 Case study II: the milling process.

In this situation, we set the length of the evaluation window as $T_r = 0.9$ s. Accordingly, the threshold values are selected as $J_1^{\text{th}} = 0.55 \times 10^{-3}$, $J_2^{\text{th}} = 0.6 \times 10^{-3}$. Figure 2 demonstrates the simulation result when m_1 and m_2 occur simultaneously, which validates the effectiveness of the proposed method with rough-memory.

Remark 10. The faults considered in the simulation are small compared with disturbance. It can be seen that the proposed geometric approach has good fault diagnosis performance, which shows that it has application potential for the detection of incipient faults. The detection of incipient faults based on the geometric approach is still an open and challenging problem that requires further research.

5.2 Case study II

In this subsection, we take an actual system model motivated by the control of chatter during the milling process to further illustrate the FDI performance of the proposed method. As can be seen in Figure 3, the milling machine has two blades that are used to cut material from a workpiece. m_1 and m_2 are the masses of the blade and tool, k_1 and k_2 are the stiffness of the two springs, ε is the damping coefficient, ϕ is the angular position of the blade, and β depends on the particular material and the used tool. In this simulation, β is set to 70°. For more details of the model, refer to [43, 44]. After making some

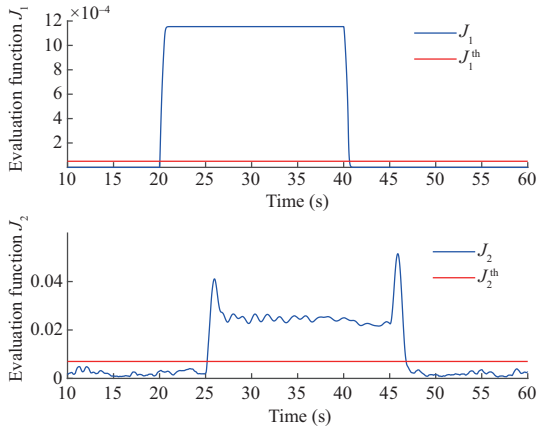

Figure 4 (Color online) Case study II: evaluation function with exact-memory when faults m_1 and m_2 occur simultaneously.

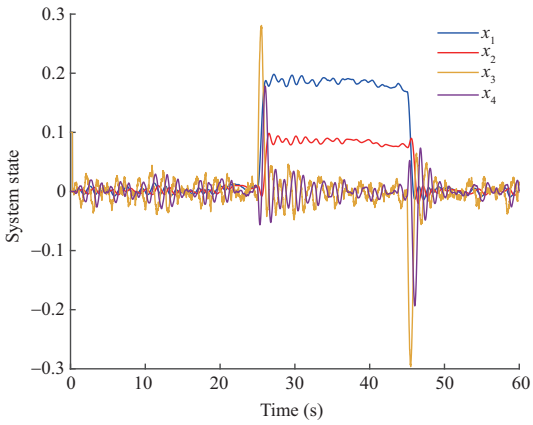

Figure 5 (Color online) Case study II: system states when faults m_1 and m_2 occur simultaneously.

modifications, we can get the system model as follows:

$$\dot{x}(t) = \begin{bmatrix} 0 & 0 & 1 & 0 \\ 0 & 0 & 0 & 1 \\ -10.34+\rho & 10 & 0 & 0 \\ 5 & -15 & 0 & -0.25 \end{bmatrix} x(t) + \begin{bmatrix} 0 & 0\,0\,0 \\ 0 & 0\,0\,0 \\ 0.34-\rho & 0\,0\,0 \\ 0 & 0\,0\,0 \end{bmatrix} x(t-\tau(t)) + \begin{bmatrix} 0 \\ 0 \\ 0 \\ 1 \end{bmatrix} u(t)$$
$$+ \begin{bmatrix} 0 \\ 0 \\ -1 \\ 0 \end{bmatrix} d(t) + \begin{bmatrix} 0 \\ 0 \\ 0 \\ 1 \end{bmatrix} m_1(t) + \begin{bmatrix} 0 \\ 0 \\ 1 \\ 0 \end{bmatrix} m_2(t),$$
$$y(t) = \begin{bmatrix} 1\,0\,0\,0 \\ 0\,1\,0\,0 \\ 0\,0\,1\,0 \\ 0\,0\,0\,1 \end{bmatrix} x(t),$$

where $\rho = \cos(2\phi + \beta)$. The time delay $\tau(t)$ is approximated to be π/ω where ω is the rotation speed of the blade. According to [43], it is assumed that $\rho \in [-1, 1]$ and $|\dot{\rho}| \leqslant 2 \times 1000 \times 2\pi/60$ rad/s, $\omega \in [200 \times 2\pi/60, 1000 \times 2\pi/60]$ rad/s and $|\dot{\omega}| = 1000 \times 2\pi/60$ rad/s^2. The system disturbance is set to $d(t) = \sin(10t)\delta(t)$ during the simulation period and the initial condition is set to $[0.1, 0, 0.1, 0]^{\mathrm{T}}$. In this simulation, we still consider there are two faults which are set as

$$m_1(t) = \begin{cases} 0.1, & 20\,\text{s} < t \leqslant 40\,\text{s}, \\ 0, & \text{otherwise}, \end{cases} \quad m_2(t) = \begin{cases} 1, & 25\,\text{s} < t \leqslant 45\,\text{s}, \\ 0, & \text{otherwise}. \end{cases}$$

These two faults exist simultaneously between 25–40 s.

In this case, we consider that the time-delay is exactly known, and the observer matrices can be obtained by verifying the matrix inequalities (15) over a grid of 65 points. The evaluation window is set to $T_r = 0.5$ s and the threshold values are set to $J_1^{\text{th}} = 5 \times 10^{-5}$, $J_2^{\text{th}} = 7 \times 10^{-3}$. The simulation results are shown in Figures 4 and 5. It can be seen from Figure 5 that, compared with fault m_2, the impact of fault m_1 on the system is very small and almost negligible. However, the proposed method can still effectively achieve the detection and isolation of these two faults, which shows the effectiveness of our method.

6 Conclusion

This paper has investigated the FDI problems for state time-delay LPV systems with external disturbance. The core concepts related to the geometric approach, such as invariant subspaces and unobservability subspaces, have been proposed for time-delay LPV systems, and the corresponding calculation algorithms have also been given. The geometric approach has been successfully introduced to the time-delay LPV systems. In this paper, two cases, where the time-delay was known and the time-delay was unknown, have been considered. FDI observers have been designed for both cases based on the geometric approach and H_∞ techniques, respectively. Wirtinger's inequality has been employed to reduce conservatism when we design the observer matrices. With the proposed geometric FDI observers, fault detection and fault isolation can be performed simultaneously. Finally, simulation examples have been presented to show the validity and effectiveness of the proposed approach. Future research topics include the following aspects: (1) generalizing and applying the geometric approach to other complex systems, such as networked control systems with network-induced delay; (2) investigating better Lyapunov-Krasovskii functionals and inequalities to further reduce conservatism.

Acknowledgements This work was supported by National Natural Science Foundation of China (Grant No. 61733009), National Key Research and Development Program of China (Grant No. 2022YFB25031103), and Huaneng Group Science and Technology Research Project.

References

1 Straka O, Punčochář I. Distributed design for active fault diagnosis. Int J Syst Sci, 2022, 53: 562–574
2 Huang D R, Hua X X, Mi B, et al. Incipient fault diagnosis on active disturbance rejection control. Sci China Inf Sci, 2022, 65: 199202
3 He X, Guo Y Q, Zhang Z, et al. Active fault diagnosis for dynamic systems. Acta Autom Sin, 2020, 46: 1557–1570
4 Hu J, Wang Z D, Liu G P. Delay compensation-based state estimation for time-varying complex networks with incomplete observations and dynamical bias. IEEE Trans Cybern, 2022, 52: 12071–12083
5 Pang Z H, Xia C G, Zhai W F, et al. Networked active fault-tolerant predictive control for systems with random communication constraints and actuator/sensor faults. IEEE Trans Circuits Syst II, 2022, 69: 2166–2170
6 Zou L, Wang Z D, Hu J, et al. Communication-protocol-based analysis and synthesis of networked systems: progress, prospects and challenges. Int J Syst Sci, 2021, 52: 3013–3034
7 Zhang Z, He X. Active fault diagnosis for linear systems: within a signal processing framework. IEEE Trans Instrum Meas, 2022, 71: 3505009
8 Qin L G, He X, Yan R Y, et al. Active fault-tolerant control for a quadrotor with sensor faults. J Intell Robot Syst, 2017, 88: 449–467
9 Wang Y A, Shen B, Zou L. Recursive fault estimation with energy harvesting sensors and uniform quantization effects. IEEE CAA J Autom Sin, 2022, 9: 926–929
10 Bu X Y, Dong H L, Wang Z D, et al. Non-fragile distributed fault estimation for a class of nonlinear time-varying systems over sensor networks: the finite-horizon case. IEEE Trans Signal Inf Process over Networks, 2019, 5: 61–69
11 Cao F F, Zhang Z, He X. Active fault isolation of over-actuated systems based on a control allocation approach. IEEE Trans Instrum Meas, 2022, 71: 3513410
12 Cai M, He X, Zhou D H. Performance-improved finite-time fault-tolerant control for linear uncertain systems with intermittent faults: an overshoot suppression strategy. Int J Syst Sci, 2022, 53: 3408–3425
13 Gao C, Wang Z D, He X, et al. Fault-tolerant consensus control for multiagent systems: an encryption-decryption scheme. IEEE Trans Automat Contr, 2022, 67: 2560–2567
14 Xue T, Ding S X, Zhong M, et al. An integrated design scheme for SKR-based data-driven dynamic fault detection systems. IEEE Trans Ind Inf, 2022, 18: 6828–6839
15 Zhang J F, Zhang Q H, He X, et al. Compound-fault diagnosis of rotating machinery: a fused imbalance learning method. IEEE Trans Contr Syst Technol, 2020, 29: 1462–1474
16 Mukaidani H, Xu H. Robust SOF Stackelberg game for stochastic LPV systems. Sci China Inf Sci, 2021, 64: 200202
17 Weiss Y, Allerhand L I, Arogeti S. Yaw stability control for a rear double-driven electric vehicle using LPV-H_∞ methods. Sci China Inf Sci, 2018, 61: 070206
18 Duan G R. Fully actuated system approaches for continuous-time delay systems: part 1. Systems with state delays only. Sci China Inf Sci, 2023, 66: 112201
19 Liu W Y, Bai Y J, Jiao L, et al. Safety guarantee for time-delay systems with disturbances. Sci China Inf Sci, 2023, 66: 132102
20 Hou T, Liu Y Y, Deng F Q. Stability for discrete-time uncertain systems with infinite Markov jump and time-delay. Sci China Inf Sci, 2021, 64: 152202
21 Han Y T, Xu Z, Guo H. Robust predictive control of a supercavitating vehicle based on time-delay characteristics and parameter uncertainty. Ocean Eng, 2021, 237: 109627
22 Tasoujian S, Salavati S, Franchek M A, et al. Robust delay-dependent LPV synthesis for blood pressure control with real-time Bayesian parameter estimation. IET Control Theor Appl, 2020, 14: 1334–1345
23 Zhang X P, Tsiotras P, Knospe C. Stability analysis of LPV time-delayed systems. Int J Control, 2002, 75: 538–558
24 Hassanabadi A H, Shafiee M, Puig V. Actuator fault diagnosis of singular delayed LPV systems with inexact measured parameters via PI unknown input observer. IET Control Theor Appl, 2017, 11: 1894–1903
25 Hamdi H, Rodrigues M, Mechmeche C, et al. Observer-based fault diagnosis for time-delay LPV descriptor systems. IFAC-PapersOnLine, 2018, 51: 1179–1184
26 Xu F, Tan J B, Wang X Q, et al. Generalized set-theoretic unknown input observer for LPV systems with application to state estimation and robust fault detection. Int J Robust Nonlinear Control, 2017, 27: 3812–3832

27 Massoumnia M A. A geometric approach to the synthesis of failure detection filters. IEEE Trans Automat Contr, 1986, 31: 839–846
28 Massoumnia M A, Verghese G C, Willsky A S. Failure detection and identification. IEEE Trans Automat Contr, 1989, 34: 316–321
29 Bokor J, Balas G. Detection filter design for LPV systems—a geometric approach. Automatica, 2004, 40: 511–518
30 Balas G, Bokor J, Szabo Z. Invariant subspaces for LPV systems and their applications. IEEE Trans Automat Contr, 2003, 48: 2065–2069
31 Basile G, Marro G. Controlled and Conditioned Invariants in Linear System Theory. Englewood Cliffs: Prentice Hall, 1992
32 Meskin N, Khorasani K. Robust fault detection and isolation of time-delay systems using a geometric approach. Automatica, 2009, 45: 1567–1573
33 Meskin N, Khorasani K. Fault detection and isolation of distributed time-delay systems. IEEE Trans Automat Contr, 2009, 54: 2680–2685
34 Meskin N, Khorasani K. A geometric approach to fault detection and isolation of continuous-time Markovian jump linear systems. IEEE Trans Automat Contr, 2010, 55: 1343–1357
35 Seuret A, Gouaisbaut F. Wirtinger-based integral inequality: application to time-delay systems. Automatica, 2013, 49: 2860–2866
36 Park P G, Ko J W, Jeong C. Reciprocally convex approach to stability of systems with time-varying delays. Automatica, 2011, 47: 235–238
37 Yang X Q, Yin S, Kaynak O. Robust identification of LPV time-delay system with randomly missing measurements. IEEE Trans Syst Man Cybern Syst, 2018, 48: 2198–2208
38 Yang X Q, Huang B, Gao H J. A direct maximum likelihood optimization approach to identification of LPV time-delay systems. J Franklin Institute, 2016, 353: 1862–1881
39 Bayrak A, Tatlicioglu E. A novel online adaptive time delay identification technique. Int J Syst Sci, 2016, 47: 1574–1585
40 Ren X M, Rad A B. Identification of nonlinear systems with unknown time delay based on time-delay neural networks. IEEE Trans Neural Netw, 2007, 18: 1536–1541
41 Wu F, Grigoriadis K M. LPV systems with parameter-varying time delays: analysis and control. Automatica, 2001, 37: 221–229
42 Briat C, Sename O, Lafay J F. Memory-resilient gain-scheduled state-feedback control of uncertain LTI/LPV systems with time-varying delays. Syst Control Lett, 2010, 59: 451–459
43 Hu Y M, Duan G. H_∞ finite-time control for LPV systems with parameter-varying time delays and external disturbance via observer-based state feedback. J Franklin Institute, 2019, 356: 6303–6327
44 Zope R, Mohammadpour J, Grigoriadis K, et al. Delay-dependent H_∞ control for LPV systems with fast-varying time delays. In: Proceedings of the 2012 American Control Conference, Montreal, 2012. 775–780